94-5-477

DEUTSCHES ELEKTRONEN-SYNCHROTRON

DESY 94-047
March 1994

Comparison of Cone and Event-Decomposition Jet Algorithms in Resolved Photon Reactions

A. Valkarova

Nuclear Center, Charles University, Praha, Czech Republic

G. Knies

Deutsches Elektronen-Synchrotron DESY, Hamburg

ISSN 0418-9833

NOTKESTRASSE 85 - 22603 HAMBURG

DESY behält sich alle Rechte für den Fall der Schutzrechtserteilung und für die wirtschaftliche Verwertung der in diesem Bericht enthaltenen Informationen vor.

DESY reserves all rights for commercial use of information included in this report, especially in case of filing application for or grant of patents.

To be sure that your preprints are promptly included in the
HIGH ENERGY PHYSICS INDEX,
send them to (if possible by air mail):

DESY **Bibliothek** **Notkestraße 85** **22603 Hamburg** **Germany**	**DESY-IfH** **Bibliothek** **Platanenallee 6** **15738 Zeuthen** **Germany**

DESY 94-047
March 1994

ISSN 0418-9833

Comparison of Cone and Event-Decomposition Jet Algorithms in Resolved Photon Reactions

Alice Valkarova
Nuclear Center, Charles University, Praha, Czech Republic

Gerhard Knies
Deutsches Elektronen Synchrotron DESY, Hamburg, Germany

March 18, 1994

Abstract: The method of jet construction by event decomposition is tested and compared to the jet construction method by cone forming. Its potential for recovering parton kinematics from large p_t and from photon remnant jets is investigated in detail. Effects from the response of a realistic detector (H1) are included. The hard scattering parton kinematics can be reconstructed with comparable quality as in the cone method. The reconstruction of the photon remnant jet mass by event decomposition provides clear advantages in comparison with the cone method for separating direct and resolved photon reactions.

1 INTRODUCTION

Investigations of low Q^2 ep interactions - photoproduction with quasi-real photons - offer at HERA a wide spectrum of interesting physics. In photoproduction the first measurement of the parton distribution function of the photon at small x is expected [1, 2, 3]. In lowest order QCD the final state is characterized by 2 jets coming from a hard scattering process. For hard processes with $p_t \leq$ 15 GeV/c contributions where the photon is resolved into quarks and gluons (resolved contribution) dominate by an order of magnitude [1, 2] in comparison with those where the photon couples directly to the partons in the proton (direct contribution).

The identification of the resolved processes will be possible by observing the photon remnant,i.e. hadrons due to the hadronization of those photonic partons not scattered by the hard process. This photon remnant can form a jet. It was proposed [2] to tag events on the existence of this photon remnant jet. For the kinematics of HERA ep collisions most particles of the proton spectator jet will remain in the beam pipe. Intrinsic transverse momentum of partons in the photon, initial state gluon radiation and colour forces cause the photon remnant particles to get out of the beam pipe and to be detected.

The photon remnant forms a low p_t jet. The UA1 cone algorithm [4] is dedicated to searching for large p_t jets from hard scattering and is therefore not designed to study remnant jets. A "extended" method for finding resolved photon remnants was proposed [5]: after finding high p_t jets with UA1 algorithm one can define a cone around the electron direction and take all hadrons there as the photon remnant jet. In direct processes only the scattered electron should be in this cone.

The JADE algorithm [6] can deal with low p_t jets. However this algorithm employs a scaled measure (so called y_{cut}) which is designed to decide on whether 2 jets should be combined into one or not. This makes sense if all the jets in an event are the result of one hard scattering process, leading to a common mass scale for all jets. Therefore the JADE algorithm is unsuitable for an isolation and measurement of the photon remnant jet.

Here we study how well parton level can be reconstructed by the method of event decomposition into jets (DECO) [7] which allows to reconstruct jets with any p_t and any mass. We present here the results of a detailed comparison obtained by the DECO algorithm and the " UA1 extended" method for both photon remnant jets and high p_t jets. A comparison of JADE, UA1 and DECO algorithms in the analysis of direct photon processes (which have no remnant) showed that JADE gave worse results for jet reconstruction than DECO [8] and it is not investigated here.

2 The jet construction algorithms

2.1 The event decomposition method

The event decomposition method starts with the full event as an entity. Jets are made by splitting the event into parts in a suitable way, by *decomposition*. There are two key elements of event decomposition:

1. a measure of jettiness in terms of an *all-event topological function* F
2. a solution finding algorithm in terms of a *minimizer* for the topological function.

The topological function is calculated from all N particles of the event with regard to their assignment to L jets, or, equivalently, with regard to the decomposition of the event into L jets. The purpose of the topological function is to adopt an extremum (actually: a minimum) :

$$F = minimum$$

when the decomposition of the event is optimal.

In the case of jets as remnants of hard partons,"optimal" means that the reconstructed jets should represent the closest kinematic approach to the original (almost) massless and hard partons. Hadronization converts some of the parton momentum into jet mass. The kinematic properties at the parton level can be taken as motivation for the following topological functions:

1. The sum of the jet masses or of the square of the jet masses should approach 0 :

$$F = \sum_{J=1}^{L} M_J, \qquad or \qquad F = \sum_{J=1}^{L} M_J^2$$

2. The sum of the jet momenta (in the event CMS) divided by the invariant mass of the event has to approach 1 . This quantity will be referred to as *L-dimensional covariant thrust* T_L [1] and yields the topological function

$$F = 1 - T_L, \qquad T_L \equiv 1/M \sum_{J=1}^{L} ((P_J P)^2/M^2 - P_J^2)^{1/2}$$

Here P and P_J are the 4-momenta of the full event and of jet J, respectively. M and M_J are their masses.

All three topological functions are Lorentz invariant. Which one is the best choice is not clear a priori, and may depend on the specific problem or purpose of the jet making.

This way, an event can be decomposed directly into any jet multiplet. It just requires an economic strategy to find the minimum configuration. The algorithm DECO provides such decompositions into jet multiplets up to the level $L = 5$. Selecting the "best" jet multiplicity for an event is decoupled from the jet making.

2.2 The UA1 cone method

This jet making algorithm starts out by finding clusters with relatively large E_t

$$E_t = \sum_{i=1}^{n} E_{ti}$$

where E_{ti} is the energy flow of particle i transverse to the collision direction, and n the number of particles in a cell in the (η, φ) space (η is the pseudorapidity and φ is the azimuthal angle). Any cell with $E_t > E_{ini}$ initiates a cluster. If the transverse energy summed up inside a cone $\sqrt{\Delta\eta^2 + \Delta\varphi^2} < R$ around the initiator cell is larger than E_{tcut}, the cone is accepted as jet. The number of cones found is the jet multiplicity of the event.

3 Comparison of jet algorithms

3.1 The test events

For the comparison of the jet algorithms we used simulated tagged ep photoproduction events in the resolved photon channel which in lowest order leads to a 4 jet configuration (two spectator jets (photon and proton) and two high p_t "actor" jets) and direct photon channel with 3 jet configuration

[1] This is the covariant form of a variable which is also known under the name "generalized thrust".

(proton spectator jet and two "actor" jets). Test events were generated with the help of the PYTHIA and HERWIG programs.

The hadronic fragmentation of the partons in PYTHIA 5.6 [9] follows the Lund string model as implemented in JETSET 7.3 [10] while HERWIG 5.5 [11] contains a different scheme of fragmentation called cluster hadronization. The incoming partons were generated in PYTHIA using the photon structure function in the GRV-LO parameterization [12]. In HERWIG simulation the photon structure function parametrization by Drees and Grassie [13] was used. Photon emission by the electron beam was treated in the Weizsäcker-Williams approximation.

Parton reconstruction via jets is distorted by initial state radiation and by multiple parton parton scattering processes. In the programs HERWIG and PYTHIA the effects of the initial and final state QCD radiation are described by leading logarithm parton showers. The multiple parton parton interaction processes are not included in these versions of Monte Carlo programs [2].

Events generated by PYTHIA and HERWIG were fed into the H1 detector [14] simulation program H1SIM and subjected to the reconstruction program H1REC. Thus we obtain samples of events similar to those which we obtain in the experiment H1. Our results are based only on the analysis of the information from the calorimeter.

3.2 How we compare DECO and UA1 algorithms

One of the aims of jet making can be to reconstruct parton kinematics. We compare the performance of decomposition (DECO) and cone method (UA1) in this respect using generated test events sample.

In the process of jet finding with DECO we proceeded in the following way: We decompose events with the help of topological function thrust [3] . For 3-jet multiplet decomposition the jet with smallest polar angle θ (relatively to the proton direction) is assumed to be the rest of the proton spectator jet and particles from this jet are excluded from the further analysis.

In the next stage the scattered electron is taken to participate in the process of decomposition (in the data the electron is measured in the electron tagger). The backward missing energy E_{miss} (due to particles lost close to the beampipe) is taken into account as a pseudoparticle with components

$$p_{miss} = (0, 0, -E_{miss}, E_{miss})$$

where $E_{miss} = E_\gamma - 1/2(\sum_{i=1}^{n} E_i - \sum_{i=1}^{n} p_{zi})$ where i runs over all calorimeter clusters (except for the electron e') and $E_\gamma = E_e - E_{e'}$. We take the 3-jet decomposition for the further analysis. The jet $J_{e'}$ containing the scattered electron is taken as the candidate for the photon spectator jet J_R (actually : $J_R = J_{e'} - e'$). In the case where there is only the scattered electron e' and the backward missing pseudoparticle in the jet $J_{e'}$, we consider this event as a direct photon event candidate and we remove this event from the analysis. The two other jets j_1, j_2 are assumed to be jets from the hard parton process. To ensure this we analyzed only events where the p_t of each jet was larger than 5 GeV/c .

The jets are matched to the scattered partons a, b. We choose the smaller value of the two possible distances of the jets j_1, j_2 to parton partners a, b.

$$R_{1a}^2 + R_{2b}^2 \qquad or \qquad R_{1b}^2 + R_{2a}^2$$

where $R_{1a} = (\eta_1 - \eta_a)^2 + (\varphi_1 - \varphi_a)^2$, and so on. Here η (φ)are the pseudorapidities (azimuthal angles) of jets and partons [4] correspondingly.

[2] Note that the effects of multiple interactions are not significant in the case when both "actor" jets have the pseudorapidities $\eta < 1.5$.

[3] M^2 gave slightly and M gave significantly worse results.

[4] Other measures for matching (e.g.$\Delta\varphi$ only, opening angle) give very similar results for the matching partons and jets.

The UA1 algorithm has 3 parameters, the energy threshold for jet initialization by a cell E_{ini}, the width of the cone R, and the energy threshold for jets E_{tcut}. The latter two together control the jet multiplicity, and R in addition the kinematic properties of the jets. We took standard values $E_{ini} = 1.5GeV$, $E_{tcut} = 7.0GeV$ and $R = 1.0$ [5]. We used a cell grid of 24 φ and 25 η bins, covering the pseudorapidity range $\eta \in (-2.5, 2.5)$.

In the cases where we found 2 jets with the UA1 algorithm we proceed in the same way as in the DECO algorithm, i.e. we assigned partons to jets by matching them with the help of the R distance. In the cases where only one jet was found we searched for the parton closest to this jet. When more than 2 jets were found we use the 2 jets with largest p_t components (which should correspond to hard process jets).

We included backward missing energy via a pseudoparticle in the same way as for DECO. We summed up all particles (clusters) collected in a cone around the electron direction to a vector which defines the photon remnant jet. The aperture of cone is chosen to include all particles for which $\eta < min(\eta_{j1}, \eta_{j2}) - \Delta\eta$. We used $\Delta\eta = 1$. If we found no activity in the backward region (except for the backward missing pseudoparticle) this event is taken as direct photon event and we remove it from the analysis of the photon remnant jets.

3.3 The reconstruction of photon remnant jets and the comparison of algorithms

In Fig.1 the difference between the azimuthal angle of generated (by HERWIG) photon remnant partons and the azimuthal angle of reconstructed (by DECO) photon remnant jets is plotted. In the case when the photon remnant jet has small p_t its azimuthal angle φ is not very well defined. Therefore we also show on this figure the same difference for jets with $p_t > 2GeV/c$. The correlation in azimuthal angle between partons and photon remnant jet is in this case better - the full width at half height is now $\Delta\varphi \sim 1.0$ (as compared to a 1.5 in Fig 1a)) with much lower pedestal. We conclude that the transverse direction of the reconstructed photon remnant jet is correlated with the partonic level even at these relatively small values of p_t.

Next we show on Figs. 2 and 3 the distributions of the laboratory polar angle θ, and of the momentum components p_t and p_z for the photon remnant at the partonic level (first row), after jet reconstruction (by DECO) in H1 detector (second row), and correlation plots for partons vs jet (third row). These distributions are shown for both HERWIG (Fig. 2) and PYTHIA (Fig. 3) generated events. At the partonic level both generators produce the remnants mainly with small p_t, backward angles θ in laboratory system and, correspondingly, negative p_z. There are also tails to larger p_t and into the forward direction. In these "tail events" the mass of photon remnant at the partonic level is large - typically 15 GeV or more. For such events DECO is not able to reconstruct correctly the remnant jets because already partons from the photon remnant and from actor (or proton remnant) parton cascades overlap. We see in the correlation plots that the partons produced with polar angles less than 150° or p_t larger than 4 GeV/c are not correlated to the reconstructed jets. The p_z distribution of jets shows differences for the models and these differences are correlated with differences at partonic level.

In Fig.4 are shown the differences between jet and partonic level pseudorapidities, azimuthal angles, and $E - p_z$ values, of the photon remnant jets from DECO and PYTHIA generated events. Here the full line is the whole sample of events, the dashed line is the subsample of events with ≥ 2 jets in UA1 method and in dotted line distributions additionally about 24 % of events are excluded because they have no remnant in UA1 method . From Fig.4 we conclude that the higher E_t cut in the cone method for actor jets selects a sample for which remnant kinematics are slightly better reconstructed with DECO but it also rejects about 60% of events from the analysis.

On Fig. 5 the distributions from DECO and UA1 are compared for this subsample of events

which is marked by the dotted line on Fig. 4. The pseudorapidity and $E - p_z$ of photon remnant jets are reconstructed with similar quality in both methods. The tails of pseudorapidity differences towards positive values are due to the fact that neither DECO nor UA1 method reconstruct photon remnant jets from partons going into the forward direction (see also comments to Figs. 2,3). The azimuthal distribution ($\Delta\varphi$) shows that remnant jets reconstructed by DECO are better correlated with the partonic level than those from UA1. The crossed distributions show that jets with a small difference in $\Delta\varphi$ are also better correlated in the other two quantities for both methods.

The photon remnant mass offers a handel for separating resolved and direct photon processes, the latter one leading ideally to $m_{JR} = 0$. Fig.6 shows the remnant jet mass distribution as reconstructed for resolved and direct photon events, respectively, by the DECO and the extended UA1 method, as measured under H1 conditions. The most striking difference between the two methods is the different fraction of $m_{JR} = 0$ jets they yield from resolved events. If in an analysis these events with remnant mass small (< 0.5 GeV) are classified as direct photon events, 29% of original resolved photon events contaminate the direct event sample in the UA1 method and only 4.8% in DECO. The ratio of true direct photon events to background is then 0.55 in UA1 method and 1.1 in DECO (see Fig. 6).

3.4 The comparison of algorithms for high p_t jets

We compare the parton reconstruction between UA1 and DECO for all jets found by UA1. If less than 2 jets are found in the UA1 method one or both partons of the event remain unassigned for a jet. These "rejected" partons can always be matched to jets from the DECO method. We can check how reasonable the DECO reconstruction of parton kinematics is in the cases when UA1 method finds no jet.

On Figs.7 - 8 we show how well the directions of hard process partons are reconstructed by their assigned jets. We compare the difference between azimuthal angle of the parton and the jet on Fig.7 for both algorithms and both event samples PYTHIA and HERWIG. On Fig. 8 the differences between the pseudorapidity of partons and jets are plotted. The relative difference in E_t between the parton and reconstructed jet is shown on Fig. 9 .

In azimuthal parton direction is similarily reconstructed in both jet algorithms. Also the widths of pseudorapidity deviations are similar. There is however a small bias for DECO jets by ~ 0.13. Transverse energy E_t is reconstructed similarily by both algorithms in PYTHIA events, while HERWIG simulation shows a small advantage for the cone method.

Note that with DECO we also obtained good correlation between parton and jet quantities in those cases when the jet was not found in the UA1 algorithm.

3.5 The comparison of algorithms for x_γ measurement

The study of resolved photon interactions is very important from the point of view of the study of the parametrization for the parton distribution in the photon. For the determination of the fraction of the parton momentum in the photon two methods are frequently used.

The first one uses the energy and momentum from the two actor jets and the photon energy E_γ [15]:

$$x_{act} = [(E - p_z)_{j1} + (E - p_z)_{j2}]/2E_\gamma \tag{1}$$

The second uses photon remnant jet instead of E_γ,

$$x_{shat} = s_{12}/s_{12R} \tag{2}$$

where $s_{12} = m^2(j_1, j_2)$ is the invariant mass of the actor jet system and $s_{12R} = m^2(j_1, j_2, J_R)$ is the invariant mass of the actor jets and photon remnant jet [5]. We have observed that a slightly better

way of calculating x from these three jets is via

$$x_{acr} = [(E-p_z)_{j1} + (E-p_z)_{j2}]/[(E-p_z)_{j1} + (E-p_z)_{j2} + (E-p_z)_{JR}] \quad (3)$$

The third method calculates x from the photon remnant jet and E_γ:

$$x_{rem} = 1 - (E-p_z)_J R/2E_\gamma \quad (4)$$

The first and the third method need the information from the electron tagger to calculate E_γ, the second method could be used also for untagged events [16]. In our analysis we have made use of E_γ in method 2 by recovering the backward missing energy with the help of the tagging information. This improves the results significantly.

The different methods have different sensitivity to measurement errors. In the absence of measurment errors they give the same results only if the involved partons are massless and have no intrinsic p_t. Since in the generators there is initial and final state gluon radiation and primordial p_t, none of these methods measures directly the original theoretical x_t. Already at the partonic level, x calculated from the massive remnants and massive cascades, differs from x_t by up to 20 %.

We now compare the quality of x-reconstruction of all these methods by showing $\Delta x = (x_t - x)/x_t$. We show Δx separately for events where UA1 yields at least 2 jets (to have the same event sample for UA1 and DECO) and for the others.

On Figs.10 and 11 we show for DECO and UA1 the relative deviations of $x_{act}, x_{acr}, x_{rem}$ for HERWIG and PYTHIA event samples, respectively. Formulas (1) and (3) yield similar resolution for x. They reproduce x clearly better than formula (4). Both algorithms UA1 and DECO give a similar width for Δx. Shifts occur when using formula (1) for DECO jets in both HERWIG and PYTHIA simulations, and for UA1 jets only in the latter case. There are also tails to large negative values of Δx ($\Delta x < -2.0$) which are not visible in Figs 10 and 11. These tails contain 8 - 9% of events for HERWIG generated events and about 12% (UA1 method) and 15% (DECO method) for PYTHIA events.

DECO also gives a reasonable x description for events for which the UA1 algorithm finds less than 2 jets. However Δx is here broader by 10 % (see Figs. 10,11).

The variables x_{acr} and x_{act} are independent measurements of x to the extent that different jet algorithms and different jet information are used. They can therefore be averaged. $x_{aver} = 0.5[x_{act}(UA1) + x_{acr}(DECO)]$ shows slightly smaller shifts of Δx than UA1 and slightly smaller width than DECO (Figs. 10,11).

4 Summary

1. We found that the photon remnant jet reconstructed with the event decomposition method (DECO) is kinematically correlated with the photon remnant at the partonic level. Kinematic properties of photon remnants can be investigated with this new jet algorithm and compared with model predictions.

2. The UA1 extended method for analysis of photon remnant jets is less powerfull than DECO mainly because its poorer efficiency of finding the remnant jet at all.

3. Using the remnant jet mass, the DECO method allows to select a much cleaner direct photon event sample than the UA1 extended method, by about a factor 2.

4. Hard process parton reconstruction by DECO and UA1 is quite similar. Here the cone method sometimes shows slightly better results than decomposition, but the differences between algorithms are much smaller than the differences between jets and partons and also smaller than the differences between the two event generating models PYTHIA and HERWIG.

5. DECO results of x reconstruction are comparable with those from the UA1 cone algorithm. The combined use of the two independent jet algorithms by averaging x from UA1 and DECO improves the x determination.

Acknowledgements One of the authors (A.V.) is grateful to the DESY directorate for the hospitality and to the DFG for financial support.

References

[1] G. Schuler, Theoretical aspects of low Q^2 physics at HERA, Physics at HERA,ed.W.Buchmüller and G.Ingelman, Proceedings of the Workshop, Hamburg 1991, p.461

[2] M.Drees,R.M.Goldbole, Phys.Rev.D39,169 (1989)

[3] A. Levy, Phenomenology and experimental issues in photoproduction at HERA, Physics at HERA, Proceedings of the Workshop, Hamburg 1991, p.481

[4] G. Arnison et al, Phys.Lett. 123 B (1983) 115

[5] G. D'Agostini,D. Monaldi, Identification of the High p_t Events Produced by a Resolved Photon at HERA and Reconstruction of the Initial State Parton Kinematics Physics at HERA,ed.W.Buchmüller and G.Ingelman, Proceedings of the Workshop, Hamburg 1991, p.527

[6] W. Bartel et al, Z.Phys.C, Particles and Fields 33,23 (1986)

[7] G. Knies "DECO - jet making by event decomposition", to be published.

[8] A. Valkarova,G. Knies, Comparison of Cluster, Cone and Event - Decomposition Jet Algorithms,H1-11/92-257 (1992) DESY

[9] T. Sjöstrand, PYTHIA at HERA, Physics at HERA, ed. W. Buchmüller and G. Ingelman, Proceedings of the Workshop, Hamburg 1991, p.1405

[10] T. Sjöstrand JETSET 6.3 Comp.Phys.Comm.39 (1986) 347 ibid 43 (1987) 367, T. Sjöstrand JETSET 7.3 manual

[11] G. Marchesini et al,Comp.Phys.Comm. 67 (1992) 465

[12] M. Glück,E.Reya,A.Vogt,Phys.Rev.C53 (1992) 127

[13] M. Drees,K. Grassie, Z.Physik C28, 451 (1985)

[14] H1 collaboration,The H1 detector at HERA,to be submitted to Nucl.Instr. and Meth.

[15] T.Ahmed et al,Phys.Lett B279,202 (1992)

[16] A. Valkarova,Separation of resolved photon processes and the determination of x_1, x_2 parton momentum fractions, Physics at HERA,ed.W.Buchmüller and G.Ingelman, Proceedings of the Workshop, Hamburg 1991, p.535

Figure captions

Fig 1)
The difference between azimuthal angle of the photon remnant at the partonic level and the jet reconstructed by DECO : a) all events and b) events with p_t of reconstructed photon remnant jet larger than 2 GeV/c.
Fig 2)
The distributions of polar angle θ, and momentum components p_t and p_z of the photon remnant at the partonic level (first row), of jets reconstructed by DECO (second row) and correlation plot between both (third row), for HERWIG generated events.
Fig 3)
The same as Fig 2) for PYTHIA generator.
Fig 4)
Difference of pseudorapidities (partons - jets from DECO), of azimuthal angles φ, of $E - p_z$ of photon remnant for PYTHIA generated events. Full line: all events. Dashed line: the subsample of events for which UA1 cone method gives $n_j \geq 2$. Dotted line: the subsample of events which are accepted as resolved by the UA1 method .
Fig 5)
The same distributions as in Fig 4) in the dotted line sample, for DECO (upper row) and for UA1 extended method (bottom row). Events where photon remnant jets have small azimuthal angle difference with partonic level are shown as crossed area.
Fig 6)
Photon remnant jet mass distribution, for the resolved event sample as in Fig 5) (upper row), and for the direct events expected to be produced (in PYTHIA) under the same conditions.
Fig 7)
The differences between azimuthal angles of partons and high p_t jets ($\Delta\varphi = \varphi_{part} - \varphi_{jet}$), for PYTHIA (top row), and for HERWIG (bottom row) generated events. The first, second and third figure show correspondingly results from DECO jets, from UA1 jets, and from DECO jets for partons where the corresponding jet was not found in UA1.
Fig 8)
The same as on Fig 7) for pseudorapidities.
Fig 9)
The same as on Fig 7) for relative deviations of transverse energy $\Delta E_t = (E_{tpart} - E_{tjet})/E_{tpart}$.
Fig 10)
First row: the distributions of $\Delta x_{act} = (x_t - x_{act})/x_t$, Δx_{acr} and Δx_{rem} for DECO. Second row : Δx_{act} for UA1 , Δx_{aver} calculated as $x_{aver} = 0.5[x_{act}(UA1) + x_{acr}(DECO)]$ and Δx_{acr} from DECO algorithm for events where < 2 jets were found in UA1. For HERWIG generated events.
Fig 11)
The same as in Fig 10) but for PYTHIA generated events.

Fig 1. Photon remnant azimuthal angle, HERWIG

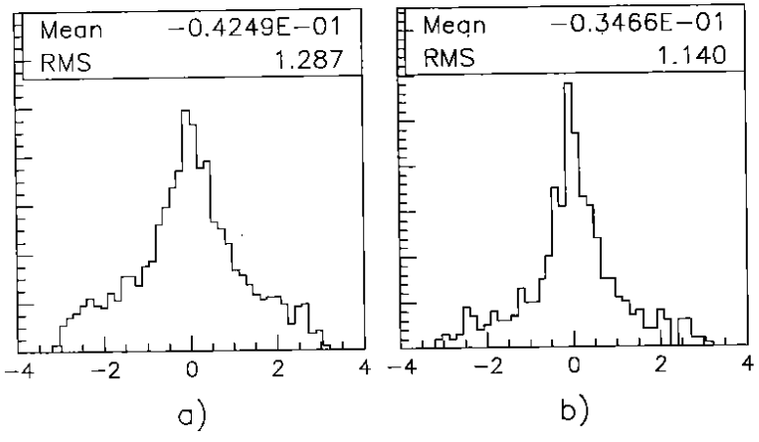

Fig 2. Photon remnant reconstruction, HERWIG

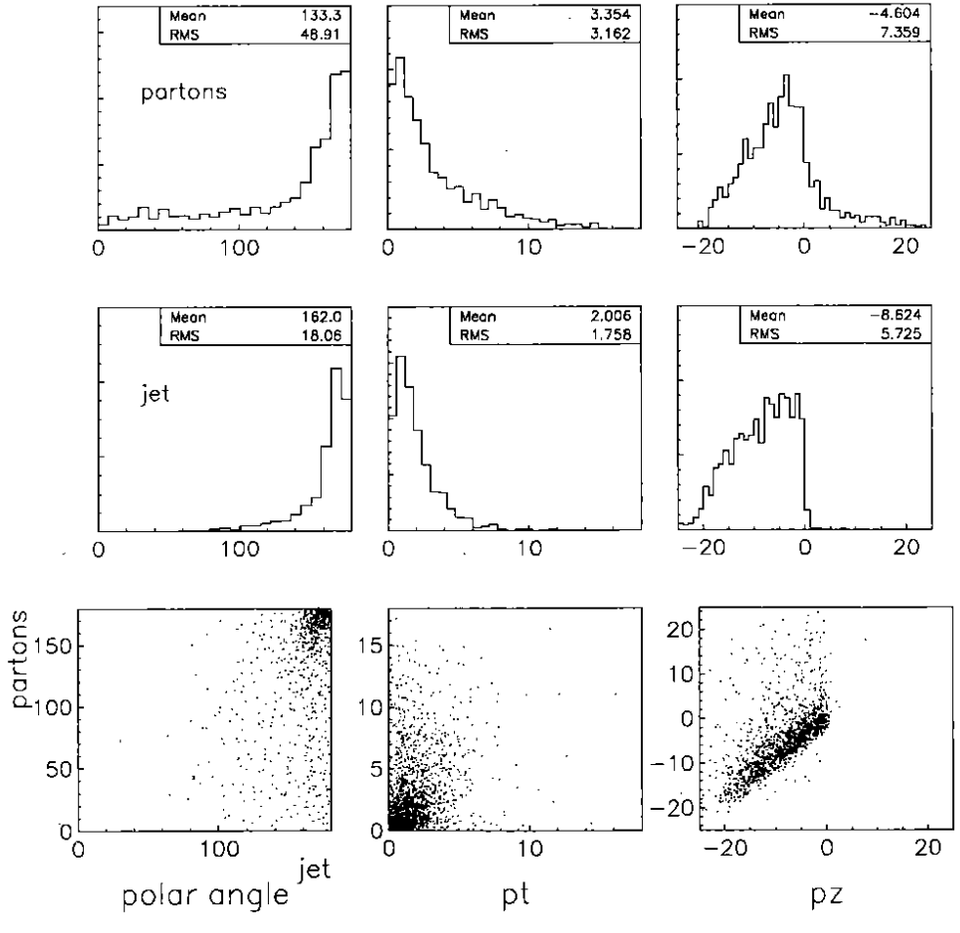

Fig 3. Photon remnant reconstruction, PYTHIA

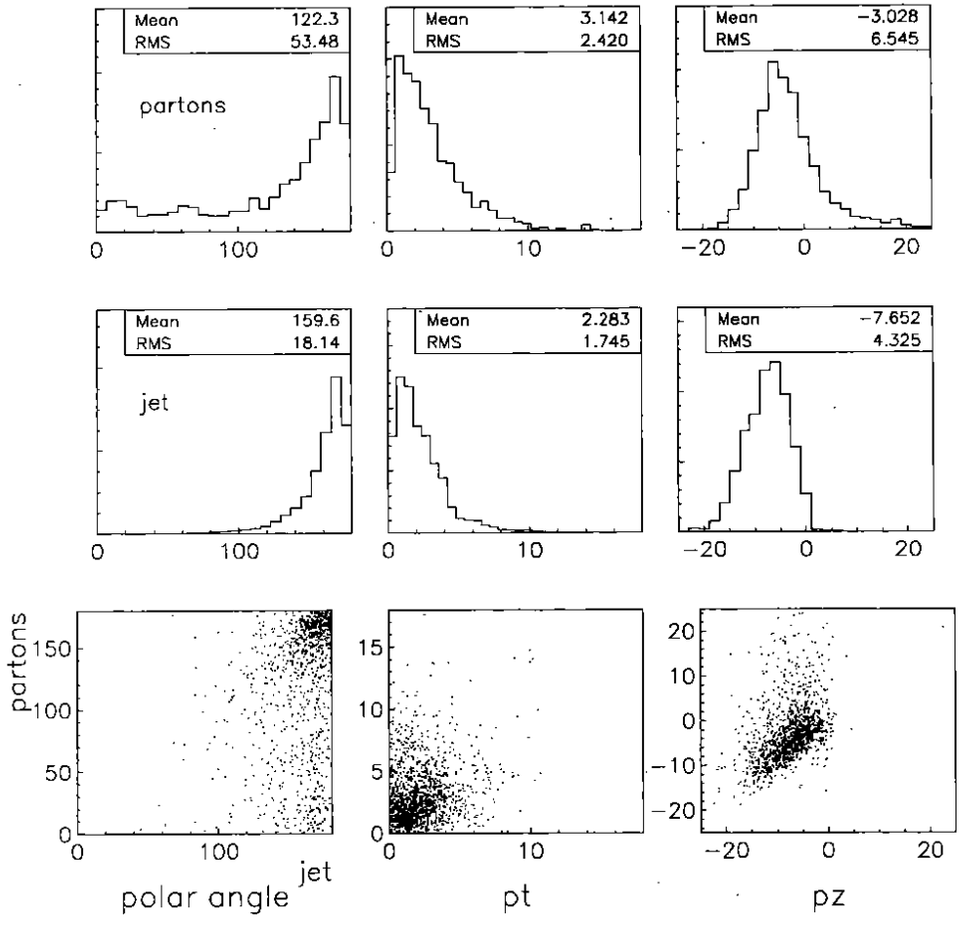

Fig 4. Photon remnant reconstruction, PYTHIA

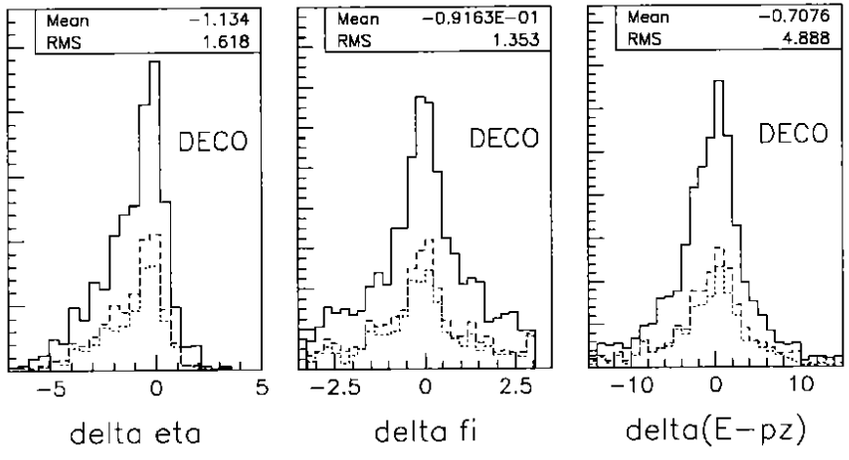

Fig 5. Photon remnant reconstruction, PYTHIA

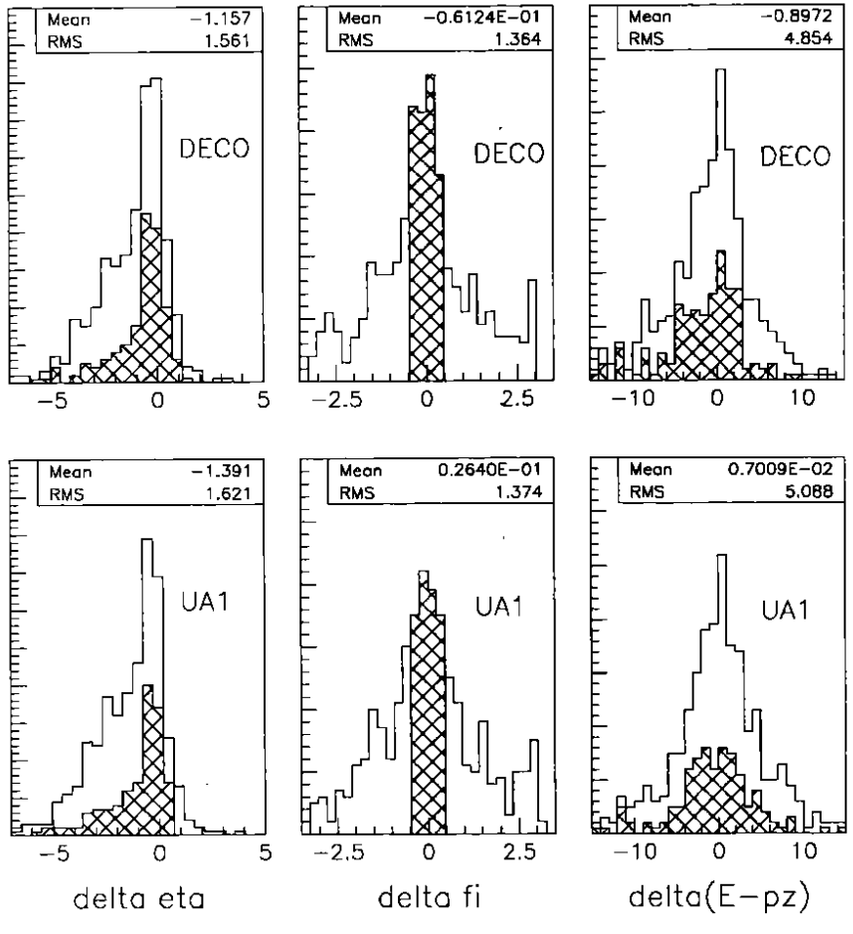

Fig 6.Photon remnant jet mass, PYTHIA

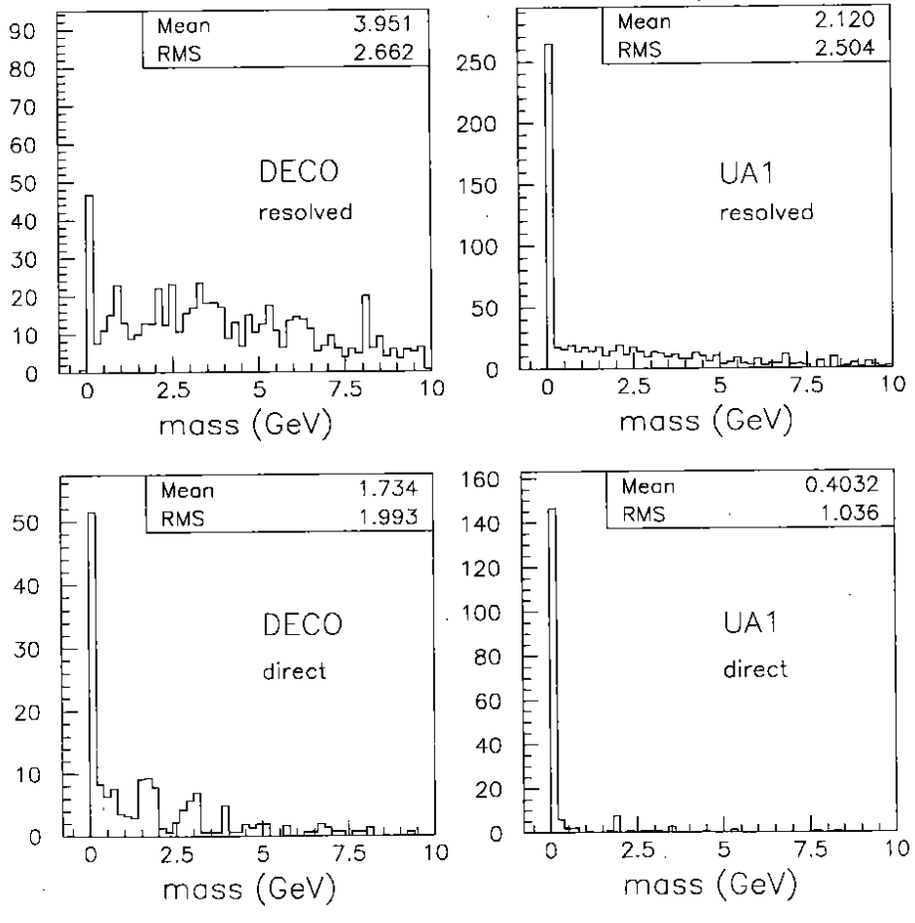

Fig 7. Azimuthal angle deviations

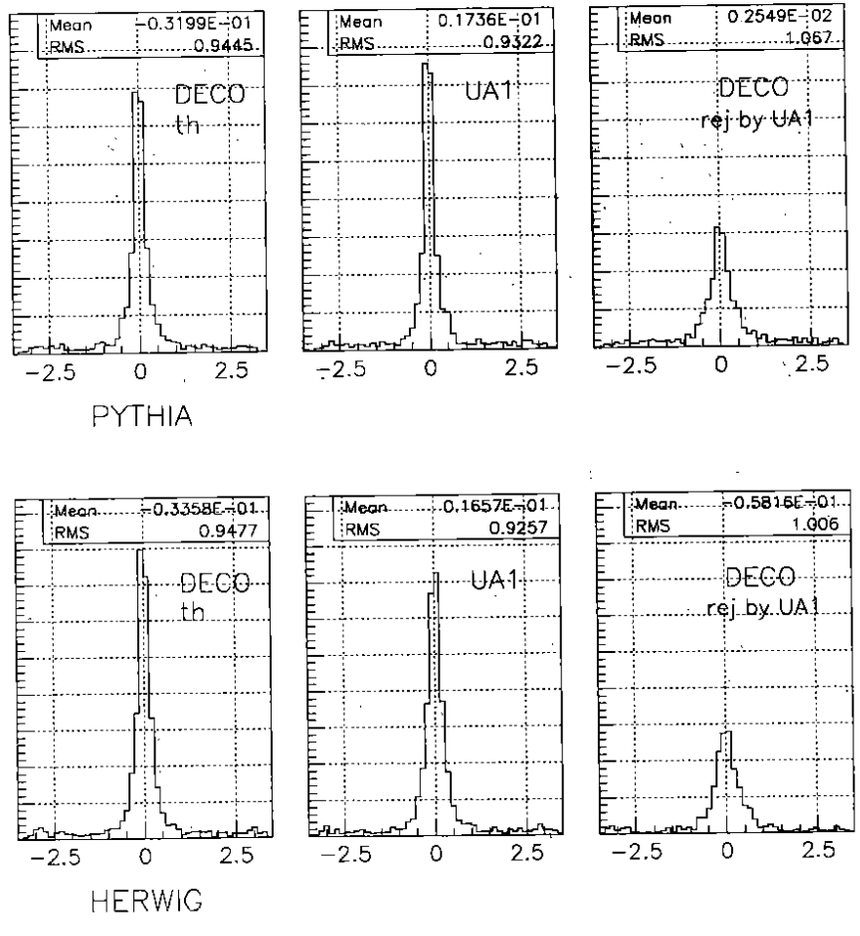

Fig.8. Pseudorapidity deviations

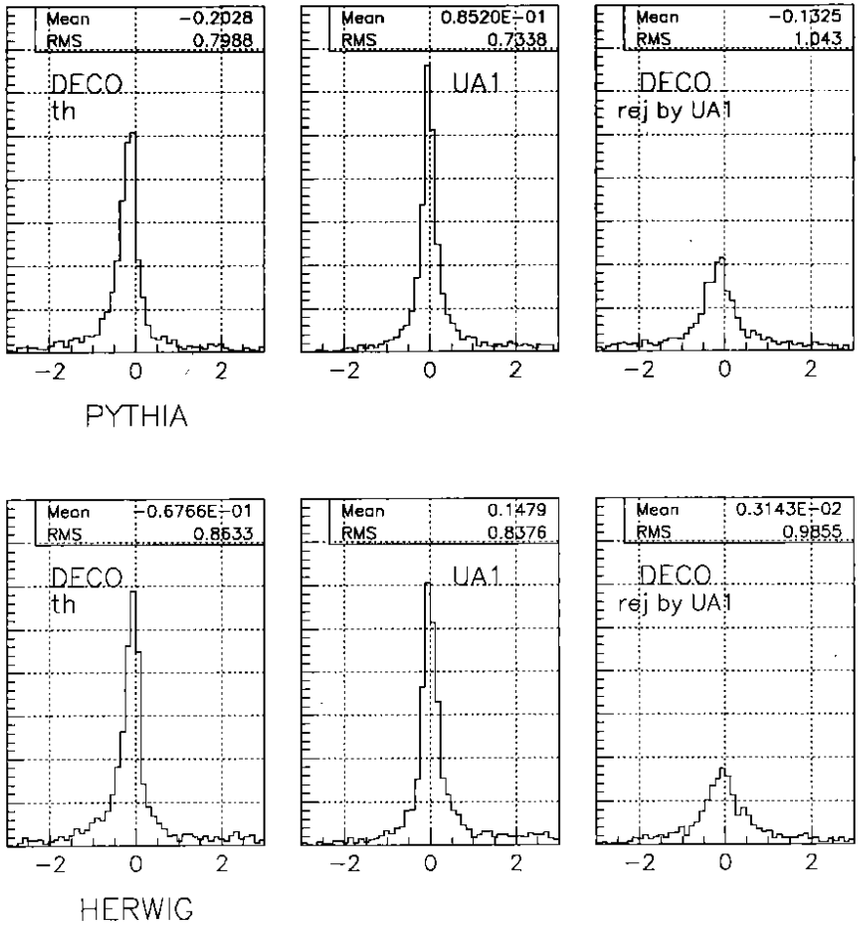

Fig.9. Et relative deviations

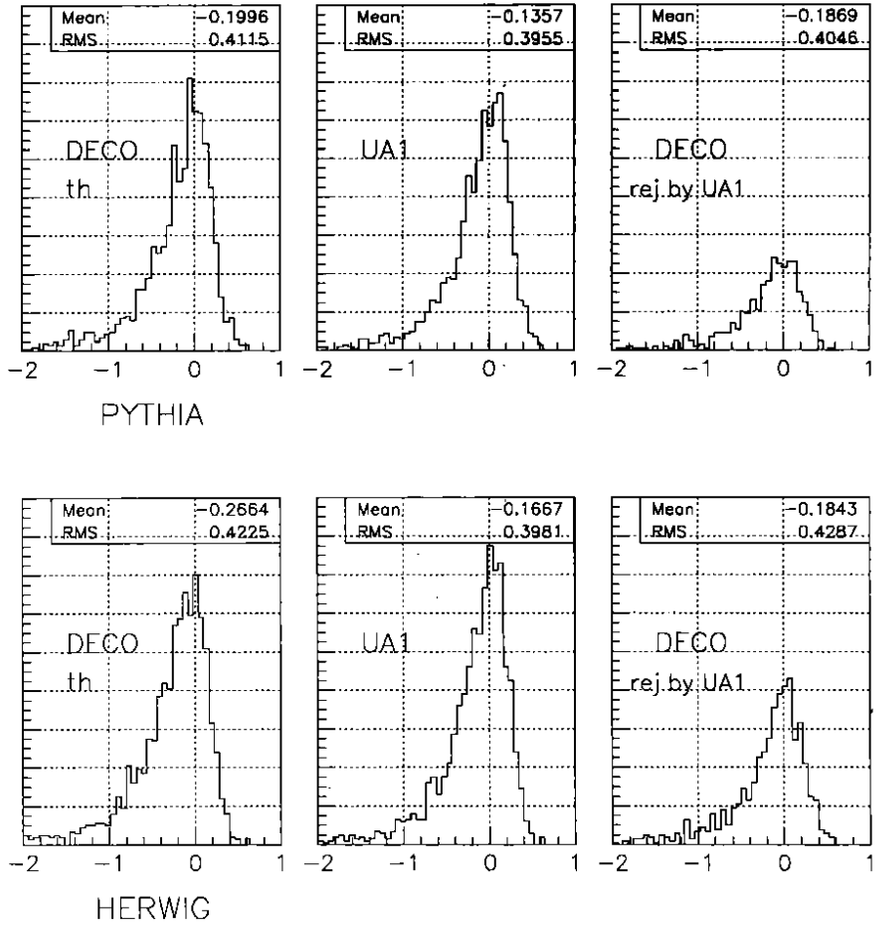

Fig 10. Delta X gamma, HERWIG

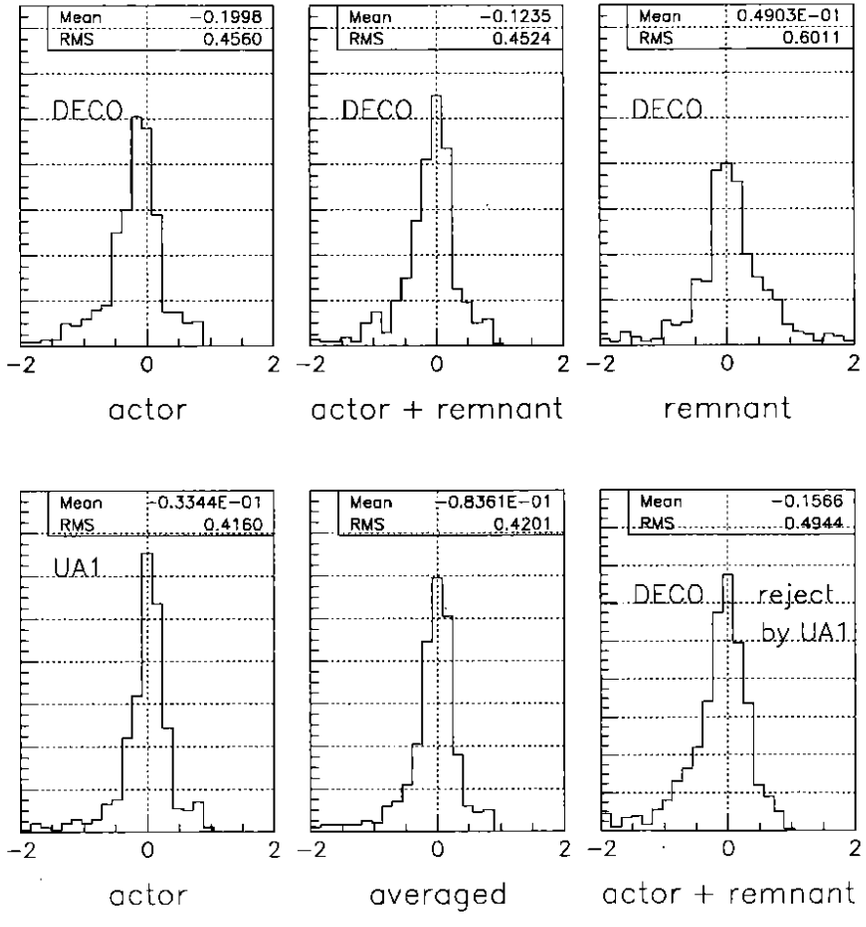

Fig 11. Delta X gamma, PYTHIA